Modelling the Dynamics of Tamponade Multi-Component Gases During Retina Re-Attachment Surgery

Sheldon K. Hall

Institute of Biomedical Engineering, University of Oxford, United Kingdom

Thomas H. Williamson

Guy's & St. Thomas Hospital. London, retinasurgery.co.uk

Jean-Yves Guillemaut

Centre for Vision, Speech and Signal Processing, University of Surrey, United Kingdom

Tony Goddard

Mechanical Engineering, Imperial College London, United Kingdom

Andrew P. Baumann, Joseph C. Hutter

United States Food & Drug Administration, Center for Devices and Radiological Health, Silver Spring MD

Vitrectomy and pneumatic retinopexy are common surgical procedures used to treat retinal detachment. To re-attach the retina, gases are used to inflate the vitreous space allowing the retina to attach by surface tension and buoyancy forces that are superior to the location of the bubble. These procedures require the injection of either a pure tamponade gas, such as C_3F_8 or

This is the peer reviewed version of the following article: [S.K. Hall, T.H. Williamson, J.-Y. Guillemaut, T. Goddard, A.P. Baumann and J.C. Hutter. Modeling the Dynamics of Tamponade Multicomponent Gases During Retina Reattachment Surgery. AIChE Journal, 63(9):3651–3662, 2017], which has been published in final form at [https://doi.org/10.1002/aic.15739]. This article may be used for non-commercial purposes in accordance with Wiley Terms and Conditions for Self-Archiving.

SF_6, or mixtures of these gases with air. The location of the retinal detachment, the anatomical spread of the retinal defect, and the length of time the defect has persisted, will determine the suggested volume and duration of the gas bubble to allow re-attachment. After inflation, the gases are slowly absorbed by the blood allowing the vitreous to be re-filled by aqueous. We have developed a model of the mass transfer dynamics of tamponade gases during pneumatic retinopexy or pars plana vitrectomy procedures. The model predicts the expansion and persistence of intraocular gases (C_3F_8, SF_6), oxygen, nitrogen, and carbon dioxide, as well as the intraocular pressure. The model was validated using published literature in rabbits and humans. In addition to correlating the mass transfer dynamics by surface area, permeability, and partial pressure driving forces, the mass transfer dynamics are affected by the percentage of the tamponade gases. Rates were also correlated with the physical properties of the tamponade and blood gases. The model gave accurate predictions in humans.

Keywords: mass transfer, perfluoropropane, sulphur hexafluoride, rates, intraocular pressure, retina

Introduction

The annual incidence of rhegmatogenous retinal detachment has been reported to be 10-18 per 100,000 with a prevalence of 0.7%[1,2]. Its onset can be rapid, with symptoms such as a sudden appearance of floaters, light flashes, blurred vision, and/or reduced peripheral vision. A detached retina can result in permanent blindness.[3] This condition can be treated by a variety or combination of scleral buckling, pars plana vitrectomy, or pneumatic retinopexy[1]. Both vitrectomy and pneumatic retinopexy can use tamponade gases. The retina is re-attached by buoyancy and surface tension forces resulting from the presence of the gas

bubble.[4] As reported by the US Medicare Part B database over 2000-2010, the use of vitrectomy has been increasing while pneumatic retinopexy use has remained stable[1]. Vitrectomy requires removal of vitreous before the gas is injected, while in pneumatic retinopexy, a gas bubble is directly injected into the vitreous. In these procedures, the intraocular gas bubble (SF_6, C_2F_6, or C_3F_8) may or may not be mixed with air depending on whether it is post-vitrectomy (usually non-expansive) or in pneumatic retinopexy were pure gas is injected where maximum expansion occurs.[4] Once the retina is in position, cryopexy or laser treatment is used to seal the detachment.[5]

The gas dynamics in pneumatic retinopexy or vitrectomy are similar. In pneumatic retinopexy, initially 100% tamponade gas is injected. The gas bubble first expands to equalize the partial pressures of nitrogen, oxygen, and carbon dioxide with the blood gas partial pressures. After reaching a maximum volume, the gases are slowly re-absorbed by the body over 12-38 days. By positioning the head, the buoyant gas bubble allows the retina to re-attach as retinal adhesion is achieved over 7-14 days, by positioning the bubble where the hole exists to reduce the inflow of fluid into the sub-retinal space through the retinal hole.[4] In vitrectomy, non-expansive gas mixtures are used, and just like in the pneumatic retinopexy case, gases are re-absorbed by partial pressure driving forces into the blood.[6,7]

In 2002, one of us developed a mathematical model of the mass transfer, pressure, and fluid flow dynamics of tamponade gases injected into the eye[7]. This earlier model was not validated for predicting gas composition or intraocular pressure in rabbits; however, it predicted gas expansion, and persistence reasonably well in the rabbit. The early model could be applied to humans, but it was not fully validated to predict expansion, intraocular pressures, and gas composition. We have since improved the model, accounting for geometric differences between the rabbit and human eye, correcting the partial pressure driving forces,

and improving the numerical solution methods. These changes gave a more accurate assessment of the multi-component mass transfer and hydrodynamics in the eye. The model was successfully used to predict some available human data of half-lives and intraocular pressure (IOP). Observations were also made about the permeability of the retina to the different gases used in pneumatic retinopathy and the dependence on the size of the tamponade gas molecules and the compositions of the gas.

Methods

To predict the dynamics of gas injected into the vitreous space, we first wrote material balances on all of the gas components: tamponade gases, oxygen, nitrogen, and carbon dioxide. We used a force balance to model the gas pressure and fluid hydrodynamics in the eye. These model equations were then fitted to published data in rabbits and the model was scaled-up to predict the dynamics in humans.

Model description

In dilute aqueous systems, such as low solubility gases in water, multicomponent mass transfer can be successfully modelled using a mass transfer coefficient and concentration driving force.[8] Others have found that reasonable results can be achieved by measuring the mass transfer of oxygen, and using similar values for the mass transfer coefficients of other components, such as nitrogen, CO_2, and/or other components to predict multi-component gas dynamics. This approach has been successful in the design of high purity oxygen waste water treatment systems.[8,9] A similar situation exists in the eye during retina re-attachment surgery, low

aqueous solubility gas mixtures are absorbed into blood. These gases need to transfer through an aqueous film and various membranes to reach the blood. Components in the blood have a higher capacity for certain gases (such as oxygen) due to hemoglobin and bicarbonate (CO_2), but the net transfer rate is controlled by diffusion through the retina. With these mass transfer coefficients, the net mass transfer can be predicted with the appropriate equilibrium partial pressure driving forces for each component.

In the eye, the main route of mass transfer of the tamponade gas, oxygen, nitrogen, and carbon dioxide will occur by partial pressure driven exchange through the retina to the surrounding blood. In addition, mass transfer can occur by exchange of the flow of aqueous humor from the eye; however, we have estimated this effect to be small and have neglected this term. We have also neglected mass transfer through the lens and anterior surface of the eye in this model.

Eye geometry

There is a significant difference in geometry between a rabbit eye and a human eye (Figure 1)[10]. The rabbit eye has a significantly larger lens to facilitate peripheral vision and avoid predators. This fundamentally alters the ratio of retina surface area to aqueous humour and vitreous volume that is driving the dynamics of the gas bubble in the rabbit relative to the human. The geometry of the eye used in the original model of Hutter et al.[7] was a simple sphere, which did not account for the volume of the lens. In this paper a more accurate representation of surface area and volume has been developed. The model was still based on a sphere, but for highly myopic patients a longer axis and higher surface area is possible. We

did not have detailed information on the anatomical variations of the patients or rabbits so we used our spherical geometry in all cases.

To determine the surface area for mass transfer, the Visualization Toolkit[11] (VTK) was used within a Python script to calculate the volume and surface area of the bubble (see supplemental material for the Python script). This involved using the intersection of two spheres to exclude a region that represented the space occupied by the lens. The bubble geometry was approximated by first creating a sphere representing the interior of the eye Figure 2-a. The region occupied by the lens was removed with a Boolean operation, whereby the intersecting volume of another sphere was deleted Figure 2-b. The bubble was truncated with a cutting plane at some height, *h*, as measured from the top of the original sphere Figure 2-c. The resulting object yielded the volume of the bubble. The surfaces associated with the lens and the cutting plane were removed, and the remaining shell provided surface area of the bubble Figure 2-d.

We also calculated the surface area and volume by an analytical calculation of the surface area of a lune. A lune is a concave-convex area created by the intersection of two circular arcs.[12] The details of this calculation can be found in the attached supplemental material.

Both the VTK calculation and the lune calculation gave excellent agreement between surface area and volume for a changing gas bubble contacting the retina surface in the rabbit (Figure 3). We also found that the more complex geometry gave good agreement with the earlier spherical model at low volumes, but at larger gas volumes the earlier model under-predicted surface area. These calculations show that correcting the total volume of the eye, in the simple sphere model, to exclude the volume occupied by the anterior chamber and the

lens gives good agreement with the rabbit geometry. This allows the simple spherical geometry to be retained, while accounting for the different geometry in each species.

Determining Equations

The eye is represented by a sphere of radius r partially filled with liquid, the remaining volume being occupied by a mixture of air and the tamponade gas. The interface between liquid and gas is a plane intersecting the sphere at a distance h measured from the top of the sphere. Due to the dynamics of the gas bubble this interface will move along the z axis, with time t, changing the bubble volume V.

The following equations describe the multi-component mass transfer of gases through the retina.

$$\frac{dN_{O2}}{dt} = -k_{O2}a\left(\frac{N_{O2}RT}{V} - P^*_{O2}\right) \quad (1)$$

$$\frac{dN_{N2}}{dt} = -k_{N2}a\left(\frac{N_{N2}RT}{V} - P^*_{N2}\right) \quad (2)$$

$$\frac{dN_{CO2}}{dt} = -k_{co2}a\left(\frac{N_{CO2}RT}{V} - P^*_{CO2}\right) \quad (3)$$

$$\frac{dN_X}{dt} = -k_Xa\left(\frac{N_XRT}{V} - P^*_X\right) \quad (4)$$

The ideal gas law $PV = NRT$ was used to substitute for the pressure in the gas bubble. The effect of surface tension on pressure was neglected in the total pressure because our estimate by the Laplace Equation[13] predicted significant effects only at a radius of curvature around 0.6 mm (0.0009 cm^3), which is smaller than most of the bubbles used in these procedures. In

clinical practice, a typical target is up to a 1 cm^3 initial injection for retinopexy, vitrectomy cases typically target a complete fill with non-expansive gases.

In order to determine the evolution of the gas bubble volume a fluid balance is constructed for the eye. The eye is assumed to have a constant influx of aqueous humour of Q_{in} cm^3/day due to active secretion and ultrafiltration. The outflow facility of the eye through the trabecular and uveoscleral pathways is determined by the permeability K_p and the difference between the intraocular pressure and the episcleral venous pressure P_{eps}. This can be expressed as

$$\frac{dV_{\text{liq}}}{dt} = -\frac{dV}{dt} = Q_{\text{in}} - K_p\left(\frac{(N_{O2}+N_{N2}+N_{CO2}+N_X)RT}{V} + P_{\text{wv}} - P_{\text{eps}}\right), \quad 5$$

where the intraocular pressure is computed using the ideal gas law, the molar quantities for each of the gas constituents and the water vapour partial pressure P_{wv}. The total volume of the eye is considered fixed and composed of the sum of the gas bubble and liquid volumes $V_{\text{eye}} = V_{\text{liq}} + V$, which enables the differential equation to be written in terms of V.

The physiological parameters used in the model have been taken from published experimental values which are shown in Table 1. Little is known about the values of the oxygen, nitrogen, carbon dioxide, and tamponade mass transfer coefficients, k_{O2}, k_{N2}, k_{CO2}, and k_x. For this reason they must be obtained by fitting the model to experimental data. In our model, we fitted k_{O2} and k_X to experimental results in the rabbit, and then used those values to predict dynamics in humans. Using the value of k_{O2}, the values of k_{CO2} and k_{N2} were estimated from the published diffusivities in water.

Additionally, the initial conditions for this model are determined by the injected tamponade gas composition and volume $V[t=0]$, N_j and $N_X[t=0]$.

In order to solve the system of equations, a function needs to be determined for calculating the surface area of the eye in contact with the bubble area. For the rabbit eye, the surface area and volume generated by the VTK or the lune calculation can be used. For the human eye, a spherical cap is a reasonable approximation since in most retinopexy/vitrectomy situations the vitreous is filled. The patient is commonly maintained in a face-down position so that this gas bubble allows surface tension to re-attach the retina and reduce fluid behind the defect. The gas bubble has reduced contact with the intraocular lens. The volume and surface area of a spherical cap can be calculated from the following:[14]

$$V = \pi h^2 (3r - h)/3 \qquad 6$$

and

$$a = 2\pi r h \qquad 7$$

For the rabbit eye, the vitreous volume was corrected for the larger lens of the eye. The surface area per unit volume used was previously shown in Figure 3. In addition, in the rabbit experiments, the rabbits head is not fixed in a downward position. Therefore, a simple spherical cap is not an accurate representation of the surface area and volume for the gas bubble.

To evaluate the components transferred by the aqueous pathway, in an earlier version of this model we included an aqueous pathway using Henry's Law to define to the concentrations of gases in water exiting through the anterior chamber. Using this equation, we found that only 1-2% of the tamponade or other gases would exit by this pathway, and thus this term was neglected in our final model. The blood perfusion to the eye is the dominant

pathway for exchange of gases. Thus, this aqueous pathway can be neglected without significant loss in model accuracy.

Results and Discussion

Mass transfer calculations in animals or the human body can be very useful in designing or evaluating medical devices or treatments for various disease or injuries. Unlike calculations used for various processes in the chemical industry, parameters in animals or humans are often harder to define, and variable. For example, in a rabbit eye, the shape of the lens changes during accommodation depending on what the rabbit is focusing on, and this affects the volume of the vitreous, and the resulting surface area coverage of the retina during the procedure. This is less of an effect in older human patients with smaller, firmer, less supple lenses. In pseudophakic patients, this volume will be less variable. In addition, the anatomy of the rabbit eye is different from the human eye. By defining the anatomy accurately, it is possible to obtain an accurate model for multi-component mass transfer processes in animals. These types of calculations can be used to predict results in humans if the anatomical parameters are properly scaled from the animal results.

The 2002 model worked well to predict expansion and persistence of intraocular gases in the rabbit. However, we have found that the 2002 version of the model did not accurately predict published gas compositions in the rabbit. To correct this problem, we adjusted the blood partial pressure driving forces to venous values as shown in Table 2.[15] As shown, lower oxygen partial pressures are a more accurate representation of the bubble concentrations as reported by Abrams et al.[16] for SF_6 (rabbits, species un-specified, 3.5–5.0 kg, 6–96 h), and

Peters et al.[17] for C_3F_8 (New Zealand white rabbits, 2.8–4.5 kg, 6–336 h). Also, both authors report long persistence of the tamponade gases with non-zero partial pressures.

Model calibration in rabbits

The model was parameterised by adjusting the mass transfer coefficient of the tamponade gas and oxygen until the best fit of volume was achieved. The values of mass transfer coefficient k_g for the other components (CO_2 and N_2) were scaled to k_{O2} using the relative diffusivities.[18] It was found that the penetration theory of Higbie ($k_g \alpha D^{1/2}$)[19] worked best to predict the mass transfer coefficients for N_2 and CO_2. The properties of the gases are in Table 3.

The mass transfer coefficients were obtained using a nonlinear gradient free method in MatLab (Natick MA), with robust weights to reduce the impact of outliers in the data. It is also important to realise that the equations are singular when $V=0$ and $V=V_{max}$ (the maximum gas volume in the eye), i.e. when the eye is entirely full or entirely empty. This leads us to discard any results that completely empty the eye of aqueous, or stop the simulation when the eye is completely filled with vitreous.

The mass transfer coefficients were obtained from what was deemed to be the best available experimental data. There were only two sources suitable for this, and these are now detailed briefly. Published results in rabbits are generally consistent but are not exact matches. This is due to the differences in protocols between investigators as well as variations between animals. Both Lincoff et al. [20] (New Zealand red rabbits, 2.5-3.0 kg, 0-35 days, CF_4, C_2F_6, C_3F_8, C_4F_{10}) and Abrams et al.[16] used direct measurement to determine the gas volume of the bubble. Lincoff et al.[20] measured gas volume after the rabbits were euthanized by recovering the gases in a graduated pipette filled with water. Abrams et al.[16] recovered the gases and

measured the volume using a graduated syringe. We believe that these methods of volume measurements are more accurate than visual methods such as measurement of the angular extent of the bubble.[21] Using the published data of Lincoff et al.[20] we fitted the model to 0.2 and 0.3 mL injections of gas in New Zealand red rabbits (Figure 4). SF_6 data (volume & composition) was fitted to the results of Abrams et al[16] (Figure 5). This combined with the Lincoff et al.[20] data comprise the full training set used to obtain mass transfer coefficients for various perfluorocarbon and SF_6 gases. The final mass transfer coefficients, obtained from this data, are shown in Table 4

Gas composition was also fitted in rabbits using the data of Peters et al. ref Peters et al.[17] reported results with C_3F_8 as a percentage of maximum volume as well as composition. We do not expect differences between New Zealand red and white rabbits since they are the same species and only differ by pigmentation. Unfortunately, the presented results are missing information for a rigorous parameterisation of the model (Peters et al.[17] reports % of maximum volume, not an exact measurement in mL). Also, Peters et al.[17] estimated the gas volume by indirect ophthalmoscopy, a visual method that may not be as accurate as direct volume measurement. Peters et al.[17] did measure the composition of the gas bubble at various time points by direct samples and a gas chromatography method. The volume & composition vs. time curves have been normalised without information about the volume normalisation provided (we estimated the maximum volume based on the initial injected gas volume). For this reason it has been used solely as validation data for volume. The rabbit mass transfer coefficients, obtained using the training data, are used to predict the experimental results of Peters et al.[17] ref. The results are shown in Figure 6. Peters et al.[17]reported slightly less expansion and a longer time to maximum volume than Lincoff et al.,[20] but he reported gas compositions up to 336 h. The rabbits in the Peters et al.[17] experiment also appear to be in

respiratory acidosis, i.e., compromised ventilation resulting in elevated CO_2 and reduced O_2 partial pressures.[22] This could have resulted from the rabbits being under stress during the experiment, such as too aggressive sedation.[23] This condition of compromised lung function may affect the gas bubble total volume in addition to the composition. We were able to accurately fit these gas compositions by adjusting the venous gas compositions to be more accurate for respiratory acidosis (Table 2). In all other cases, we used normal venous gas compositions as noted in Table 2.

Peters et al.[17] also reports IOP measurements for rabbit experiments for a direct injection of tamponade, where vitrectomy has not been performed. This shows a characteristic spike in the IOP for the first day. Our model predicts this due to a rapid influx of water vapor, and a direct comparison is shown in Figure 7. The prediction is made using the mass transfer coefficients derived from the Lincoff et al.[20] data and a typical size for a New Zealand white rabbit eye. The predictions of intraocular pressure spikes in the human also were good and were consistent with our previous model.[7,24] Clinically, increases in IOP are usually not an issue as long as the retina remains perfused.

Predictions in humans and the features of mass transfer dynamics

Using the rabbit data to obtain mass transfer coefficients and then using them to predict human experimental results is another way to validate the model. This has been done for some of the data found in Jacobs et al.[25] (humans, air, SF_6, C_3F_8) Jacobs et al.[26] measured gas volume vs. time by A-scan ultrasound. A-scan ultrasound measures the height of the liquid bubble, and this allows calculation of the volume.[26] This method of volume measurement is likely more accurate than visual methods. Jacobs et al.[25]reported results for both vitrectomy (removal of aqueous followed by the injection of tamponade gas mixed with air) as well as

pneumatic retinopexy (pure tamponade gases injected). Jacobs et al.[25]also measured the dynamics of a direct air injection. There is good agreement for SF_6 and C_3F_8 in these retinopexy cases (Figures 8). We found that venous concentrations had to be used in the blood gases, as the arterial values were not as good of a fit. In Figures 8, we tested the human response prediction from the rabbit against the best fit we could obtain by adjusting the mass transfer coefficients. As shown, the rabbit prediction is almost the same as a best fit in a human. It is known that the retina is about 3 times thicker in the rabbit vs. the human[20], even with this difference, the mass transfer in the rabbit was a good model for what happens in the human.

As previously noted, there are two versions of this type of surgery using tamponade gases. We also applied the model to the case of vitrectomy. In this case, the initial conditions of the model are adjusted to dilute the tamponade gas with air. Usually physicians target non-expansive gas concentrations initially for these procedures (15 -17% for C_3F_8, and 18-20% for SF_6).[6] We applied the model to the literature reported cases of vitrectomy reported by Jacobs et al.[25] The results of our fits are shown in Table 5. We can fit the Jacobs et al.[25] results better by simply changing the mass transfer coefficients, we show this result for 2 typical vitrectomy cases in Figures 9 & 10 (best fit values: k_x = 1.32-1.50 x 10^{-8} & k_{O2} = 3.45-2.98 x 10^{-8} mol/cm^2-day-mmHg).

In retinopexy, there is an expansion phase - maximum - and an absorption phase. After a tamponade gas is injected, it immediately begins to diffuse out of the eye while simultaneously blood gases enter. Since the rate of gases entering exceeds the loss of tamponade, the bubble expands. At or near the non-expansive gas concentrations, the bubble reaches a maximum volume. After which the data in rabbits indicates that the bubble concentration becomes relatively stable, approximating the blood gas compositions with small amounts of tamponade gas (usually less than 10%). In the case of vitrectomy, the injected gas

contains air and tamponade, the bubble undergoes minimal to no expansion, and the gas compositions also approach the venous blood gas composition with small amounts of tamponade gas, essentially the same situation as in the retinopexy injection in the absorption phase. Thus, it would be expected that once the bubble gas compositions stabilize to a near steady state, the dynamics of the absorption should be the same whether this state was obtained by either retinopexy or vitrectomy routes.

Some features of a 0.5 cm^3 injection of pure C_3F_8 (retinopexy case in a non-vitrectomized eye) are shown in Table 6. The volumetric maximum occurs at 3.21 days, as C_3F_8 depletes and blood gases diffuse into the bubble. Initially blood gases transfer rapidly into the bubble, reaching a maximum at 3.49-3.63 days (blood gas maximums). These relative rates reflect the best fit values of the mass transfer coefficient that were adjusted relative to oxygen for both N_2 & CO_2 using the approximation of Higbie (mass transfer proportional to diffusivity$^{1/2}$). The relative maximum moles of each gas transferred are also shown in Table 6. Assigning the tamponade gas as 1.00, we found for this test case that 3.39 moles of N_2 are transferred per mole of tamponade, 0.24 moles of CO_2/mol tamponade and 0.22 moles of O_2/mol tamponade are also transferred to the bubble. Thus, nitrogen is the major gas transferred to the bubble.

As previously noted, the gas composition reaches a near steady state composition during the absorption phase, and the ½-lives of each blood gas component are nearly the same (9.7–9.8 days, then 5.9 days). The ½-lives predicted by the model are variable and change with time, but they can be approximated by a biphasic fit, with the 2nd calculated ½-life being shorter. This may be attributed to the composition of the bubble at longer times, i.e., the bubble is richer in blood gases, which are smaller molecules than the tamponade gas, and thus

diffuse faster. The tamponade gas disappears most rapidly in the earlier phases of the injection due to its higher partial pressure driving forces.

As a comparison to C_3F_8, SF_6, another commonly used tamponade, has less expansion (only 2x) in retinopexy (0.5 cm^3 injection – human) and faster dynamics relative to C_3F_8 (Table 7). However, as in the case of C_3F_8, after the volume reaches maximum, the gas composition also rapidly approaches a blood gas composition diluted with a small amount of tamponade. In this case, although the bubble has a similar composition to the C_3F_8 bubble in the absorption phase (compositions approaching the venous gas partial pressures with a small amount of tamponade gas), the gases are absorbed much faster than C_3F_8. Again, N_2 dominates the gases transferred, but only 1.58 mol N_2/mol tamponade is transferred in this case.

Previously, it has been reported that as the gas bubble expands, its dynamics is dominated by a "nitrogen equilibration".[6] The gas bubble was thought to initially undergo expansion, then nitrogen equilibration, then dissolution. In fact, the gas bubble is never in equilibrium with the blood, much less in nitrogen equilibrium.

Effect of initial gas composition

The results reported for rabbits and humans with a vitrectomy procedure indicate a slightly different trend than would be expected based on the dynamics observed in retinopexy. Table 8 shows the results of a simulation to a 3.0 mL injection of 10% C_3F_8 diluted with air. In this case, the bubble is close to a non-expansive state initially, but the air gases are richer in O_2 and poorer in CO_2 than the typical venous blood gases. So during the absorption phase in vitrectomized eyes, the bubble composition will re-adjust to balance the partial pressures of

the venous blood gases. In contrast, the volumetric ½-life predicted by the retinopexy results is also considerably shorter than would be expected for a vitrectomy (Table 8).

As reported in the literature for C_3F_8, and SF_6, the ½-lives change depending on the amount of tamponade gas in the injection.[27,28] The fitted results for these cases are shown in Table 5. For example, the ½-life of C_3F_8 increases from 4.2 days to 12.5 days as the initial C_3F_8 concentration changes from 5% to 20%. Other authors have attributed this to the low solubility of C_3F_8 in water, with lower solubilities slowing the absorption.[25] However, we have found with our model that solubility alone cannot account for this trend. If a 5% and a 20% injection were equivalent, when the 20% case reduces to 5%, one would expect the initial 20% volume rate of decrease to eventually match the 5% case. It does not. The 20% case still decreases in volume more slowly even after the tamponade gas reduces to 5%.

A typical vitrectomy case will also achieve the same state as a pneumatic retinopexy as far as gas composition and volume. In a retinopexy injection, C_3F_8 may drop to about 15% in about the first 2-3 days. At that point, the bubble is approaching about the same composition as a vitrectomy case, but the ½-life is considerably longer following vitrectomy even if the bubble compositions are similar shortly after the expansion phase in retinopexy. Also by contrast, the injection of air by itself is rapidly depleted, and our fitted mass transfer coefficients (air injection, volume ½-life = 3 days)[25] for O_2, N_2, and CO_2 are considerably larger than what was found when retinopexy cases are fitted (C_3F_8 volume ½-life = 9.88 days). We found that the tamponade mass transfer coefficients for the vitrectomy case in Table 8 had to increase about 50% relative to the retinopexy values, and the oxygen and other blood gases had to be reduced about 40% to fit the experimental data. Thus, the slower transfer of blood gases is controlling the volume dynamics in vitrectomy.

These trends cannot be fully explained by the physical properties of the gas, or possible interactions between the components that could be fitted by a more advanced treatment of the gas dynamics, such as the Maxwell-Stefan Equation. One possible explanation is that the tamponade gases themselves insult the membranes, i.e., cause some type of inflammation or biological reaction that changes the properties of the retina's membranes or changes in the intraocular blood flow. This reaction appears to be dose dependent and volume dependent, injecting a high volume of C_3F_8 and air for example in a vitrectomy, injures the membranes, relative to a lower volume retinopexy injection, and slows the transfer of the blood gases. Lower doses or no doses of tamponade, such as direct air injection, are much less tissue reactive. The membranes are then more permeable as evidenced by gas bubbles with about the same partial pressures absorbing much faster following a retinopexy exposure. The type of gas SF_6 vs. C_3F_8, also appears to have an effect.

Effect of gas physical properties

Physical properties do play a role in the mass transfer dynamics. We have observed that the rapid transfer of oxygen relative to the transfer of other blood gases correlates with its kinetic diameter (Table 9).[29,30] The kinetic diameter is the smallest effective diameter for a molecule. Oxygen is diatomic, the molecule is cigar shaped, and the kinetic diameter is controlled by its minor axis. Oxygen has a higher MW than nitrogen, 31.9980 g/mol vs. 28.0134 g/mol, but the kinetic diameter of oxygen is smaller 2.3-3.4 Å vs. 3.1-3.6 Å. (Oxygen has 8 protons, nitrogen 7, this contributes to the smaller size of oxygen.) In tire applications, it is known that O_2 permeates through rubber 3-4 times faster than N_2, which is why N_2 is used in some high performance tire applications (e.g., aircraft landing gear).[30] The reported diffusivity of oxygen in water is larger than the diffusivities of N_2 or CO_2. Based on our modelling, the

effect of kinetic diameter is not as pronounced for the retinal membranes as it would be expected for denser rubbers or elastomers.

Another factor besides the molecular size and shape is its equilibrium aqueous solubility. The literature reports that Xe gas rapidly is depleted when used as a tamponade (88% removal in 3h in rabbits).[14] Although Xe has a relatively large size (4.2 A), it diffuses from the eye due to is rapid dissolution into water. Xe has a relatively high solubility in water relative to oxygen, nitrogen, or carbon dioxide due to its smaller Henry's Law Constant (Table 10).

At very long times, all of the gas bubbles transition from a spherical cap, to a spherical bubble shape.[20] When this occurs, the transfer of gas is considerably slowed due to less surface area contact with a blood perfused tissue. This effect would cause lingering of the gas bubble at longer times.[25] We did not account for this in our model, although it would be a factor for observed persistence of the gases observed in humans or rabbits at long times.

It is also possible to examine more closely the relationship of the physical properties of the molecules to the mass transfer coefficients and look for trends that might enhance the understanding of the dynamics. Due to the sparsity of the data all of it was used (Lincoff, Abrams and Jacobs), irrespective of species, to determine parameters for the different gases for this analysis. These were then plotted against molecular volume. The plots are shown in Figures 11A & B and it is apparent that a linear relationship exists (retinopexy cases).

We also found that the mass transfer coefficients are a strong function of initial gas composition (retinopexy to vitrectomy cases) for C_3F_8, not as much the case for SF_6, with variation that can be largely attributed patient variability.

As shown in Table 5 for C_3F_8, mass transfer is most rapid for air, than slows as C_3F_8 is added. We found that the mass transfer coefficient for C_3F_8 decreased with increased gas concentration (Figure 12). There was one outlier result at 6% C_3F_8. This outlier indicates that individual patients can have very different gas absorption rates given the same relative initial gas compositions. Still, this outlier for the 6% C_3F_8 case had a mass transfer coefficient for O_2 that was only about 33% of the pure air values. The mass transfer coefficients for the blood instead showed a local minimum. Again, patient variability was large,[31-34] and it is difficult to ascertain the exact values of the mass transfer coefficient for any single patient. However, what we have quantified is the expected transfer rates and their relative possible ranges in humans. This high variability is likely a contributor to the limited success of these procedures in humans with these conditions. Chang et al.[31] reported a 55.4% successful rate of re-attachment for these procedures.

There was much less variability in the limited rabbit experiments, since these experiments were all completed under controlled conditions with healthy eyes with retinopexy.

The limited data and patient variability for SF_6 data also made it too difficult to identify specific trends; however, the composition effect appears to be much less important than the patient variability in this case.

The human variability can be attributed to many factors, such as the size/shape of the detachment, head position (always face-down vs. up-right, exposing different structures to the gas bubble), surgical variations in dosing, variations in the diseases and conditions that result in a detached retina, and variations in vitreous volume based on variations in the axial length of the eye. These disease conditions include things such as: retinal detachment with and without

proliferative vitreoretinopathy, proliferative diabetic retinopathy, macular holes, giant retinal tears, and ocular trauma.[6] Each of these disease conditions or injuries affects the structure of the remaining membranes differently (e.g., proliferative vitreoretinopathy results in proliferation of retinal pigment epithelial cells and the formation of scar tissue, diabetic retinopathy results in disruption of the blood vessels, etc.), affecting the transport properties.

Un-acceptable elevations in IOP are possible in pneumatic retinopexy if too much tamponade gas is injected into the eye. This will usually result in an immediate increase in intraocular pressure and may necessitate removal of intraocular aqueous fluid which in some techniques is removed before injecting any gas in pneumatic retinopexy. This will displace all the aqueous in the eye, and then the partial pressures of the blood gases can drive elevations in IOP. This effect was recognized by both regulatory agencies and medical device suppliers and there are warnings in product labelling that limit the maximum volumes of various injected tamponade gases. This model could predict short term elevations in IOP following injection of pure tamponade gas. The IOP in this situation is controlled by the hydraulic permeability used in the model. Elevations in IOP in patients with compromised aqueous hydraulic function, as in glaucoma, are also possible, we did not model this situation, and restricted our model to the expected dynamics in a relatively healthy eye (except for the detached retina). The IOP ranges from 12-20 mmHg in healthy humans[15] and 15-20 mmHg in rabbits.[35] The human eye can tolerate elevations of IOP to 20-30 mmHg for short periods, but pressures as high as 70 mmHg are possible in disease states such as glaucoma.[15] Our aqueous dynamics in eq. 5 were previously found to predict IOP in humans very well[7], and had the same functional form as in the literature[36] with the simplification of constant inflow. These pressure-flow equations may not be accurate in diseased states such as glaucoma.[36]

Conclusions

We improved our previously developed model for the mass transfer of tamponade gas, oxygen, nitrogen and carbon dioxide. These improvements include correcting for the larger lens in rabbits relative to humans (which affects surface area), using venous blood compositions in the partial pressure driving forces, and improving the numerical solution methods. The improved fits of rabbit data give much improved predictions of gas dynamics and compositions in both rabbits and humans. It appears that the tamponade gas exposure may affect the gas dynamics in the bubble. For example, following vitrectomy and the use of C_3F_8, the retina's membranes are less permeable to blood gases than they would be if a smaller retinopexy injection was used. Mass transfer is also controlled by the size of the molecules, and their relative partial pressures and solubilities in water/blood. The volumetric ½-life is a composite of the dynamics of all of the components.

Acknowledgements

The author's would like to recognize the significant contributions of one of our colleagues and co-authors, Tony Goddard, who passed away in 2014 before this work was finished. Tony was the first to not only recognize, but also suggest many improvements to the earlier attempts to model mass transfer in the eye. This work would not have been completed without his contributions.

The study used the computational resources of the High Performance Computing clusters at the Food and Drug Administration, Center for Devices and Radiological Health.

Disclaimer

The mention of commercial products, their source, or their use in connection with the material reported herein is not to be construed as either an actual or implied endorsement of such products by the US Food and Drug Administration.

Notation

a = surface area for mass transfer, cm^2

h = height of spherical cap gas bubble, cm

k_j= mass transfer coefficient of component j, mol/cm^2-day-mmHg, j= O_2, N_2, CO_2, x = tamponade gas, C_3F_8, C_2H_6 or SF_6

K_p = hydraulic permeability, cm^3/day-mmHg

N_j = moles of component gas j in bubble, j= O_2, N_2, CO_2, x

P^*_j = venous partial pressure of gas j, mmHg

P_{eps} = episcleral venous pressure, mmHg

P_{wv} = water vapor pressure, mmHg

Q_{in} = aqueous production, cm^3/day

R = universal gas constant, cm^3 – mmHg/mol-deg K

t = time, days

T= temperature, K

V = bubble gas volume, cm^3

V_{liq} = vitreous liquid volume, cm^3

V_{eye} = volume of eye, cm^3

1. Ahmad B, Shah G, Blinder K. Trends & Approaches to Repairing Retina Detachments. *Review of Ophth On-Line* 2013; http://www.reviewofophthalmology.com/content/d/retinal_insider/i/2355/c/40108/.
2. Haimann T, Barton T, Brown C. Epidemiology of Retinal Detachment. *Arch Ophthalmol.* 1982;100:289-292.
3. Boyd K. Retinal Detachment: Torn or Detached Retina Symptoms. 2016; http://www.aao.org/eye-health/diseases/detached-torn-retina-symptoms. Accessed August 21, 2016, 2016.
4. Chan C, Lin S, Nuthi A, Salib D. Pneumatic Retinopexy for the Repair of Retinal Detachments: A Comprehensive Review (1986-2007). *Survey of Ophthal.* 2008;53(5):443-478.
5. Kozarsky A. What is a Detached Retina? 2016; http://www.webmd.com/eye-health/eye-health-retinal-detachment#2. Accessed February 28, 2017, 2017.
6. Chang S. Intraocular Gases. *Retina.* Vol 3. St. Louis, MO: CV Mosby Co.; 1989:245-259.
7. Hutter J, Luu H, Schroeder L. A Biological Model of Tamponade Gases Following Pneumatic Retinopexy. *Current Eye Research.* 2002;25(4):197-206.
8. McWhirter J, Vahidieck N. Oxygenation System Mass Transfer Design Considerations. In: McWhirter J, ed. *The Use of High-Purity Oxygen in the Activated Sludge Process*. West Palm Beach FL: CRC Press, Inc.; 1978:235-260.
9. Roberts P, Munz C, Dandliker P. Modeling Volatile Organic Solute Removal by Surface and Bubble Aeration. *J WPCF.* 1984;56(2):157-163.
10. Short B. Safety Evaluation of Ocular Drug Delivery Formulations: Techniques and Practical Considerations. *Tox Pathology.* 2008;36:49-62.
11. Schroeder WM, Ken; Lorensen, Bill. The Visualization Toolkit, 4th ed. 2006. Accessed August 21, 2016.
12. Pantelidis L. Area of a Spherical Lune Formed by Two Random Planes. *Global J of Adv Res on Classical and Modern Geo.* 2010;1(2):85 - 88.
13. Atkins P. *Physical Chemistry.* 2nd ed: WH Freeman & Co.; 1982.
14. Lincoff A, Lincoff H, Solorzano C, Iwamoto T. Selection of Xenon Gas for Rapidly Disappearing Retinal Tamponade. *Arch Ophthalmol.* 1982;100:996-997.
15. Guyton A, Hall J. *Textbook of Medical Physiology.* 10th ed. Philadelphia PA: WB Saunders Co.; 2000.
16. Abrams G, Edelhauser H, Aaberg T, Hamilton L. Dynamics of Intravitreal Sulfur Hexafluoride Gas. *Invest Ophthal.* 1974;13(11):863-868.
17. Peters M, Abrams G, Hamilton L, Burke J, Schrieber T. The Nonexpansile, Equilibriated Concentration of Perfluoropropane Gas in the Eye. *Am J Ohthal.* 1985;100:831-839.
18. Perry R, Green D, eds. *Perry's Chemical Engineer's Handbook.* 6th ed. New York: McGraw-Hill Book Co.; 1984.
19. Bird R, Stewart W, Lightfoot E. *Transport Phenomena.* New York NY: John Wiley & Sons, Inc.; 1960.
20. Lincoff H, Maisel J, Lincoff A. Intravitreal Disappearance Rates of Four Perfluorocarbon Gases. *Arch Ophthalmol.* 1984;102:928-929.

21. Parver LML, H. Mechanics of Intraocular Gas. *Invest Ophthal & Vis Sci.* 1978;Jan:77 - 79.
22. Garcia M. Blood-Gas Analysis of Electrolytes in Rabbits. Paper presented at: Southern European Veterinary Conference; October 20-22, 2016, 2016; Granada Spain.
23. Weatherdpoon D. Respiratory Acidosis. 2015; http://www.healthline.com/health/respiratory-acidosis#Overview1. Accessed February 28, 2017, 2017.
24. Hllton GF. *Pneumatic Retinopexy and Alternative Techniques.* St. Louis, MO: CV Mosby Co.; 1989.
25. Jacobs P, Twomey J, Leaver P. Behaviour of Intraocular Gases. *Eye.* 1988;2:660-663.
26. Jacobs P. Intraocular Gas Measurement Using A-Scan Ultrasound. *Current Eye Research.* 1986;5:575 - 578.
27. Thompson JT. Kinetics of intraocular gases. Disappearance of air, sulfur hexafluoride, and perfluoropropane after pars plana vitrectomy. *Arch Ophthalmol.* 1989;107(5):687-691.
28. Thompson JT. The absorption of mixtures of air and perfluoropropane after pars plana vitrectomy. *Arch Ophthalmol.* 1992;110(11):1594-1597.
29. David Y, Paganessi J, Rufin D. Emission Reduction of Perfluorocompounds in Semiconductor Manufacture via Capture and Recycle. *Green Engineering*: American Chemical Society; 2000.
30. Murphy K. Are Nitrogen Molecules Really Larger than Oxygen Molecules? The correct answere, with respect to "permeation", is yes. 2015. Accessed Nov 5, 2015.
31. Chang S, Lincoff H, Coleman D, Fuchs W, Farber M. Perfluorocarbon Gases in Vitreous Surgery. *Ophthal.* 1985;92:651-656.
32. Hsu J, Gerstenblith A, London N, et al. *Retina.* 2014;34(12):2458-2461.
33. Kontos A, Lee J, A S, Shalagai Z, Williamson T. Duration of Intraocular Gases Folllowing Vitreoretinal Surgery. *Graefes Arch Clin Exp Ophthal.* 2017;255:231-236.
34. Thompson J, Smiddy W, Glaser B, Sjaarda R, Flynn H. Intraocular Tamponade Duraftion and Success of Macular Surgery. *Retina.* 1996;16(5):373-382.
35. Gelatt K. *Veterinary Ophthalmology.* Vol 1. 4th ed. Oxford UK: Blackwell Publishing; 2007.
36. Hart W. *Adler's Physiology of the Eye.* 9th ed. St. Louis MO: Mosby Year Book; 1992.

TABLES FOR AIChE PAPER

Table 1. Parameters used in the model.

Symbol	**Description**	**Value**
R	Universal gas constant	62,396 cm^3 mmHg mol^{-1} K^{-1}
T	Physiological temperature	310 K
r_r	Eye radius (rabbit)	0.8 – 0.95 cm
r_h	Eye radius (human)	1.2 cm
	Lens thickness (rabbit)	7.9 mm
	Lens thickness (human)	4.0 mm
	Maximum vitreous volume (rabbit)	3.0 cm^3
	Maximum vitreous volume (human)	7.0 cm^3
	Vitreous chamber depth (rabbit)	6.2 mm
	Vitreous chamber depth (human)	16.32 mm
Q_{in}	Aqueous inflow (rabbit & human)	3.2 cm^3/day
P_{eps}	Episcleral venous pressure	8 - 9 mmHg
K_p	Hydraulic permeability	0.37 cm^3/day/mmHg

Table 2 - Blood gas partial pressure used in the model.

	Venous blood in respiratory acidosis, Peters et al.[15] data mmHg	Venous blood gas partial pressure mmHg	Arterial blood partial pressure mmHg
O_2	29.8	40	104
N_2	554.1	628	569
CO_2	63.2	45	40
Tamponade	67.6	0	0
Water	47.0	47	47

Table 3 - Physical properties of intraocular gases

Gas	Molecular weight D	Molecular volume A^3 *	Oil/gas partition coefficient	Solubility in water
CF_4	88.003	255.0	0.052	---
C_2F_6	96.088	343.5	0.146	15 mg/L**
C_3F_8	188.017	418.0	0.208	5.7 mg/L**
C_4F_{10}	238.024	492.9	0.437	---
SF_6	146.052	309.1	0.280	41 mg/L**

*Calculated using QikProp v 1.6, Schrodinger, Inc. Portland OR

**XiMed product information

Table 4 – Fitted mass transfer coefficients (mol/cm^2-day-mmHg), rabbits. CF_4, C_2F_6, C_3F_8, and C_2F_{10} were fitted to Lincoff (2.5 – 3.0 kg New Zealand red rabbits), SF_6 was fitted to Abrams (3.5 – 5 kg rabbits)

Gas	Injected volume	Fitted tamponade mass transfer coefficients in rabbit	Fitted O_2 mass transfer coefficients in rabbit	Higbie predicted mass transfer coefficient N_2	Higbie predicted mass transfer coefficient CO_2
CF_4	0.20 mL	6.80e-08	1.55e-07	1.34e-07	1.34e-07
CF_4	0.30 mL	6.29e-08	2.00e-07	1.73e-07	1.73e-07
C_2F_6	0.20 mL	1.61e-08	8.30e-08	7.15e-08	7.15e-08
C_2F_6	0.30 mL	2.04e-08	1.00e-07	8.62e-08	8.62e-08
C_3F_8	0.20 mL	9.39e-09	5.63e-08	4.85e-08	4.85e-08
C_3F_8	0.30 mL	8.77e-09	5.36e-08	4.62e-08	4.62e-08
C_4F_{10}	0.20 mL	4.80e-09	3.43e-08	2.96e-08	2.96e-08
C_4F_{10}	0.30 mL	5.33e-09	3.96e-08	3.42e-08	3.42e-08
SF_6	0.85 mL	5.49e-08	1.81e-07	1.56e-07	1.56e-07

Table 5 – Fitted mass transfer coefficients (mol/cm^2-day-mmHg), human vitrectomy cases.

Gas & Purity %	Injected volume	Fitted tamponade mass transfer coefficients in human	Fitted O_2 mass transfer coefficients in human	Higbie predicted mass transfer coefficient N_2	Higbie predicted mass transfer coefficient CO_2
Air	3.8 mL	----	2.53e-07	2.18e-07	2.18e-07
Air	4.3 mL	----	1.72e-07	1.49e-07	1.49e-07
SF_6 20%	5.9 mL	7.51e-08	1.13e-07	9.73e-08	9.73e-08
SF_6 20%	4.7 mL	6.32e-08	1.63e-07	1.41e-07	1.41e-07
SF_6 20%	6.9 mL	7.97e-08	2.34e-07	2.02e-07	2.02e-07
SF_6 20%	7.9 mL	1.04e-07	1.79e-07	1.55e-07	1.55e-07
SF_6 20%	8.2 mL	9.19e-08	1.67e-07	1.44e-07	1.44e-07
SF_6 20%	9.7 mL	1.55e-07	2.43e-07	2.10e-07	2.10e-07
SF_6 20%	13.8 mL*	9.95e-08	1.81e-07	1.56e-07	1.56e-07
C_3F_8 6%	2.4 mL	2.04e-08	5.62e-08	4.85e-08	4.85e-08
C_3F_8 6%	3.5 mL	2.46e-08	6.04e-08	5.21e-08	5.21e-08
C_3F_8 6%	6.4 mL	1.03e-07	7.33e-08	6.32e-08	6.32e-08
C_3F_8 12%	5.0 mL	1.50e-08	2.98e-08	2.57e-08	2.57e-08
C_3F_8 16%	5.4 mL	1.31e-08	3.45e-08	2.98e-08	2.98e-08

*This eye was anomalously large, and it has a high mass transfer rate compared to other cases. It is not explained in Jacobs et al. ref what caused this unusual gas fill, perhaps aphakic or psuedophakic patient (no lens or intraocular lens replacement) , i.e., gas expanding into anterior chamber could account for this case.

Table 6 - Multi-component dynamics for a C_3F_8 retinopexy simulation in a human, 0.50 mL injection of 100% C_3F_8 (average of mass transfer coefficients fitted to Jacobs)

Component	Time to maximum (days)	Maximum moles gas/moles tamponade	First ½-life (days)*	2nd ½-life (days)*
O_2	3.49	0.22	9.82	5.91
CO_2	3.63	0.24	9.72	5.90
N_2	3.63	3.39	9.72	5.90
C_3F_8	0.00	1.0	0.85	1.06
Volume	3.21	---	9.88	5.97

*First ½-life was defined as the time it took for the bubble volume to decrease from maximum to 50% volume, the 2nd ½-life was the time for volume reduction between 50 – 25%.

Table 7 - Multi-component dynamics for a SF_6 retinopexy simulation in a human, 0.50 mL injection of 100% SF_6 (mass transfer coefficients fitted to Jacobs)

Component	Time to maximum (days)	Maximum moles gas/moles tamponade	First ½-life (days)	2nd ½-life (days)
O_2	0.57	0.10	2.59	1.71
CO_2	0.59	0.11	2.58	1.70
N_2	0.59	1.58	2.58	1.70
SF_6	0.00	1.0	0.11	0.13
Volume	0.47	---	2.61	1.73

Table8. Multi-component dynamics for a C_3F_8 3.0 mL vitrectomy simulation in a human, 10% C_3F_8, 71% N_2, 19% O_2.compared to a retinopexy case

Component	Literature reported retinopexy ½-life in humans (days)	½-life prediction using retinopexy mass transfer to predict vitrectomy case (days)	½-life prediction using vitrectomy mass transfer coefficients (days)
O_2	--	0.7	1.29
CO_2	--	12.15	21.29
N_2	--	12.15	21.27
C_3F_8	--	1.35	0.91
Volume	12.6	12.42	21.93

Table 9- Some physical properties that affect mass transfer

Component	MW Da	Kinetic diameter	Diffusivity in water[19]
O_2	31.9980	2.90 – 3.45 Å*	2.5×10^{-5} cm^2/s
N_2	28.0134	3.14 – 3.6	1.9×10^{-5}
CO_2	44.01	3.30	1.96×10^{-5}

*K Murray (Air Products & Chemicals), YE David ACS Symp Ser

Table 10 – Henry's Law constants and solubilities in water, P = Hx, P=partial pressure (atm), H = Henry's Law constant (atm/mol fraction), x = mol fraction in water[21;22]

Component	Henry's Law Constant H atm/mol-fraction	Temperature K	Partial Pressure atm	Predicted solubility
O_2	5.0×10^4	310	0.21	7.46 mg/L
N_2	10×10^4	310	0.78	6.06 mg/L
CO_2*	1.9×10^3	298	0.053	67.1 mg/L
Xe	1.7×10^4	310	1.0	429 mg/L

*CO_2 also is bound as bicarbonate

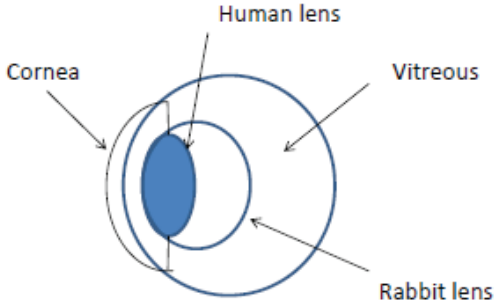

Figure 1 – Schematic diagram of geometry used in the model calculations. As shown for the rabbit, the lens occupies more vitreous volume compared to the human, which alters the surface area/volume ratio for mass transfer through the retina.

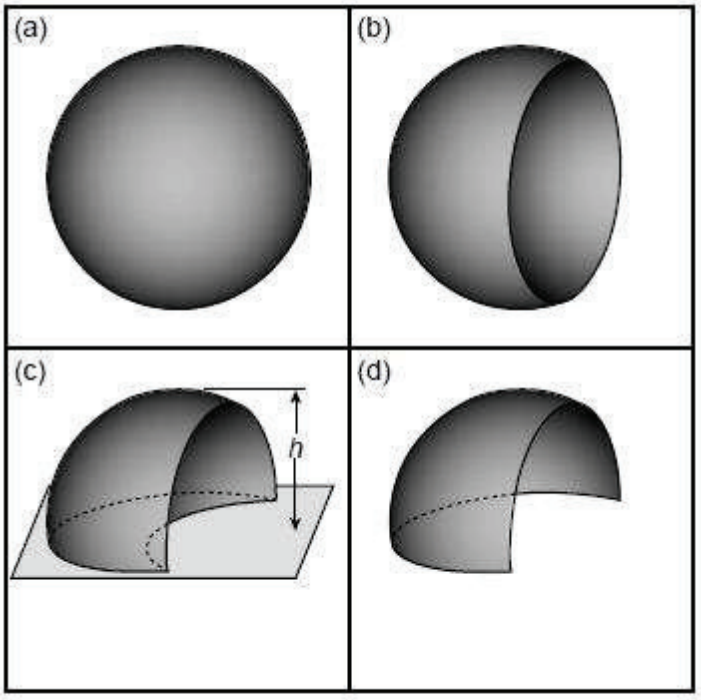

Figure 2 – A computer model (VTK) was used to calculate the volume and surface area of a bubble within a rabbit eye. (a) First, a spherical volume was created to represent the interior portion of the eye. (b) Then, the portion of the volume occupied by the lens was removed. The lens was approximated with another spherical volume. A Boolean operation was used to remove the intersection of these two spheres, thus yielding an approximation of the volume of the interior portion of the eye excluding the lens. (c) Finally, the height of the bubble was accounted for. A plane was positioned at a distance, *h*, as measured from the top of the volume. All volume below this plane was excluded. (d) Lastly, the surface area of the bubble was calculated. The lens-contacting surface and the planar bottom surface of the bubble volume were removed. The remaining shell provided the surface area of the bubble.

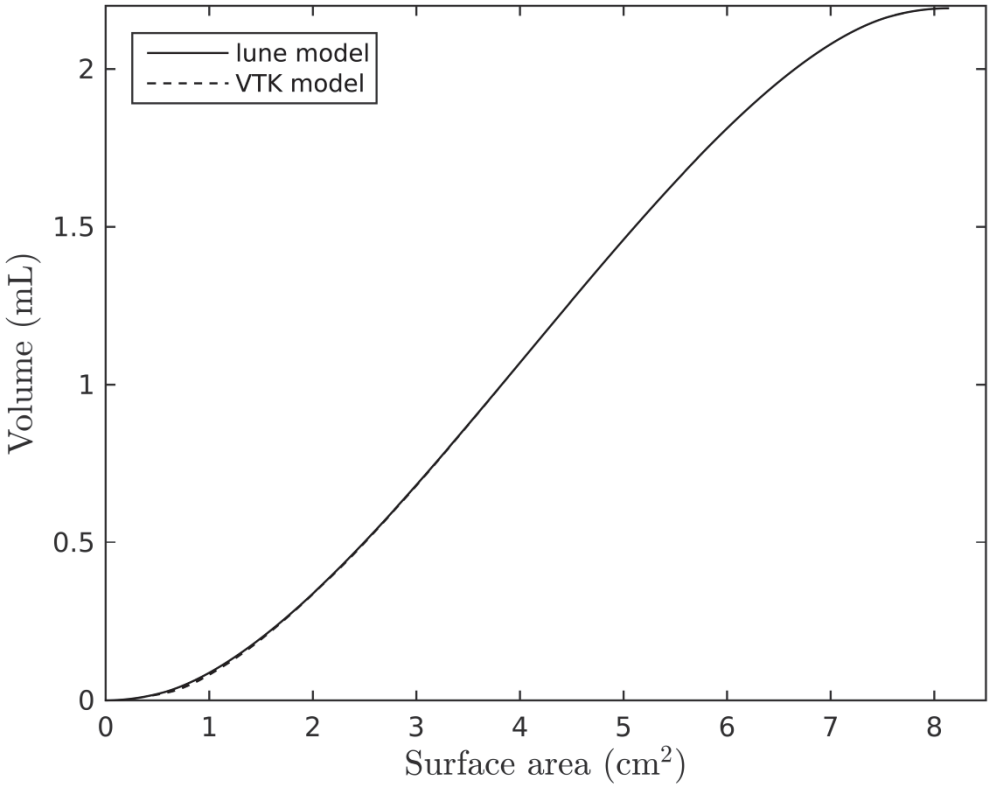

Figure 3 – Volume vs. surface area in a rabbit eye.

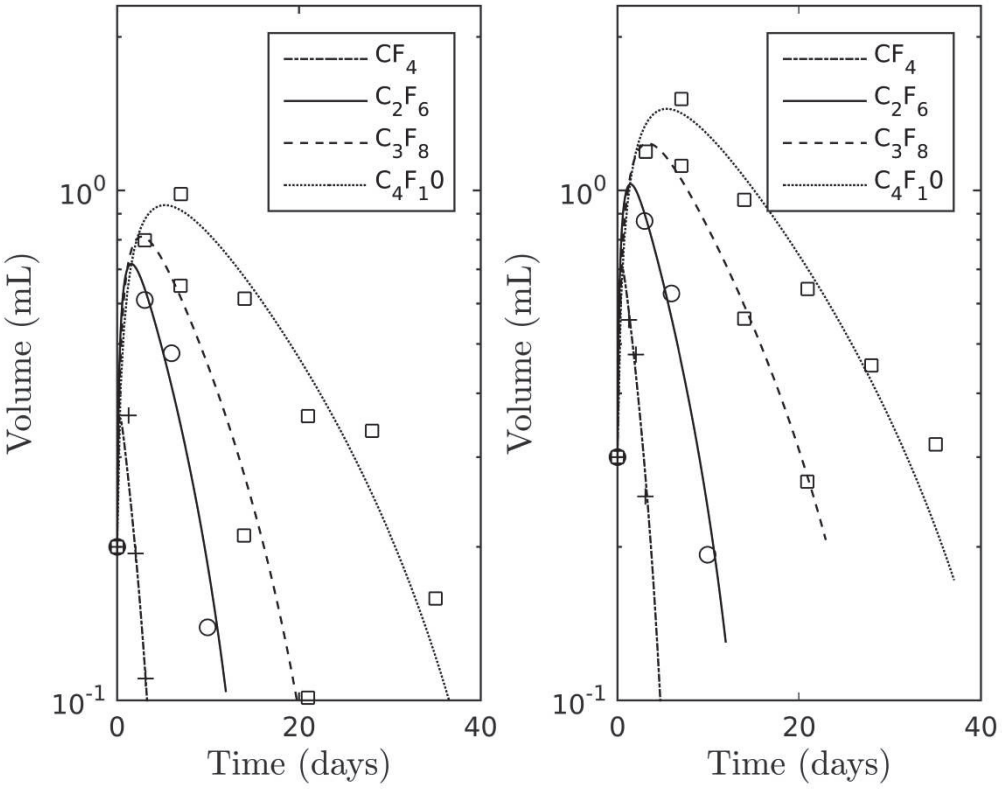

Figure 4 – Model calibration - results of the fit to Lincoff's rabbit data for CF_4, C_2F_6, C_3F_8, and C_4F_{10} (lune model with eye cavity of volume 2.2mL).

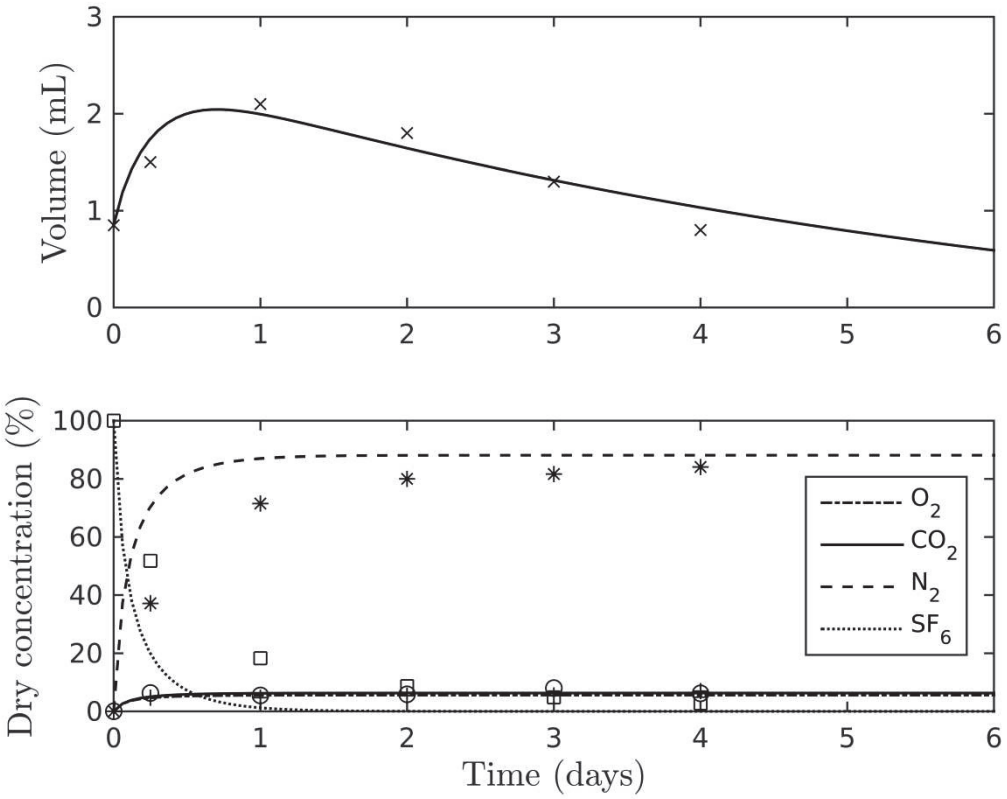

Figure 5 – Calibration of model to SF_6 results from Abrams (fitted lune model with eye cavity of volume 2.2mL) and used that to predict.

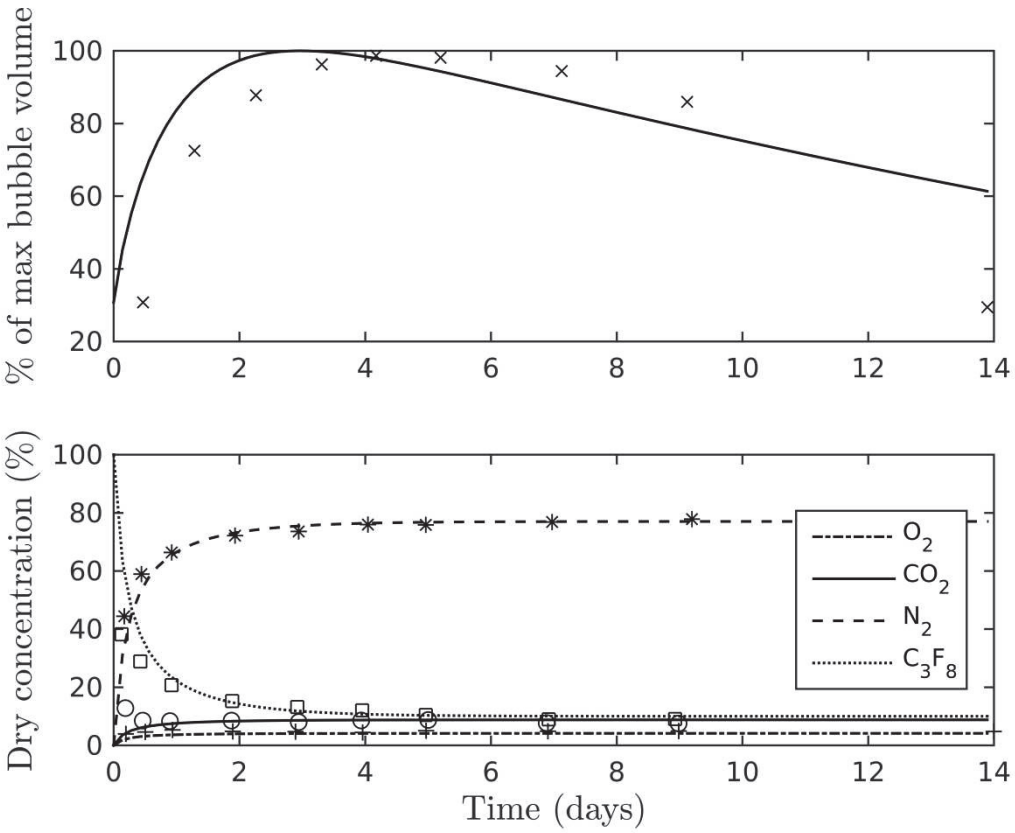

Figure 6 – Model prediction for the rabbit C_3F_8 case. The best mass transfer coefficients to the two C_3F_8 datasets from Lincoff (lune model with eye cavity of volume 2.2mL) were used to define the average mass transfer coefficient for each gas and used that to predict Peters' results (same lune model with eye cavity of volume 2.2mL).

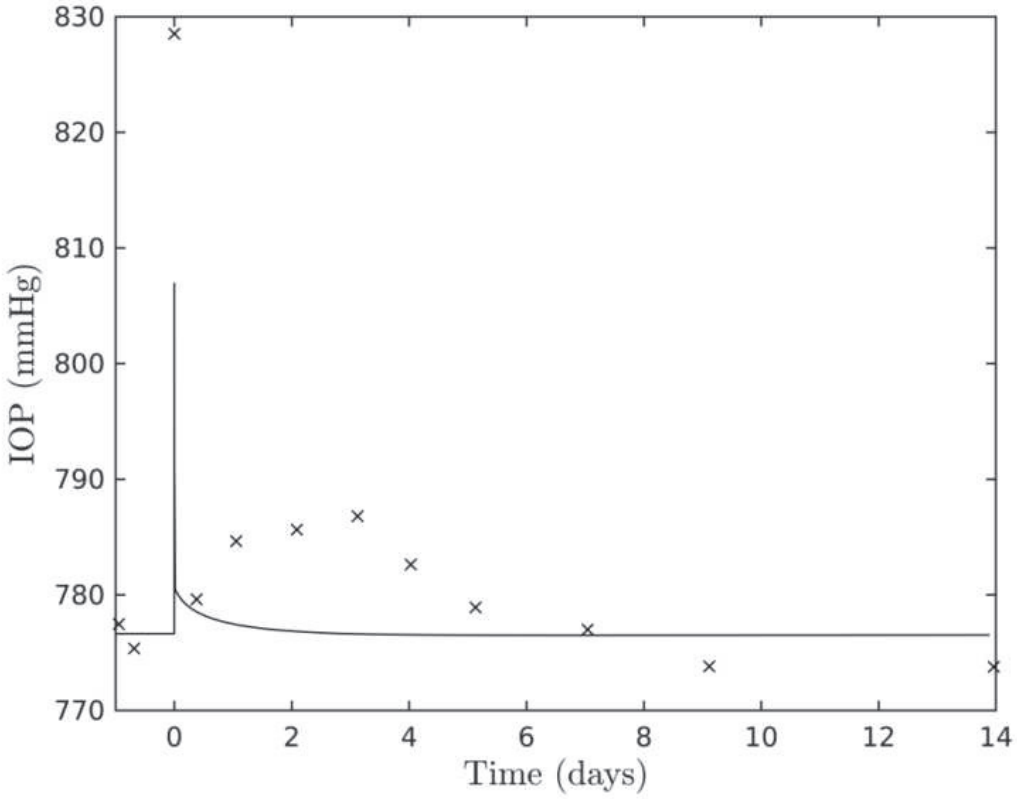

Figure 7 – Predicted IOP against measurements by Peters in a rabbit. This used the coefficients fitted to the two Lincoff C_3F_8 dataset and then averaged for each gas.

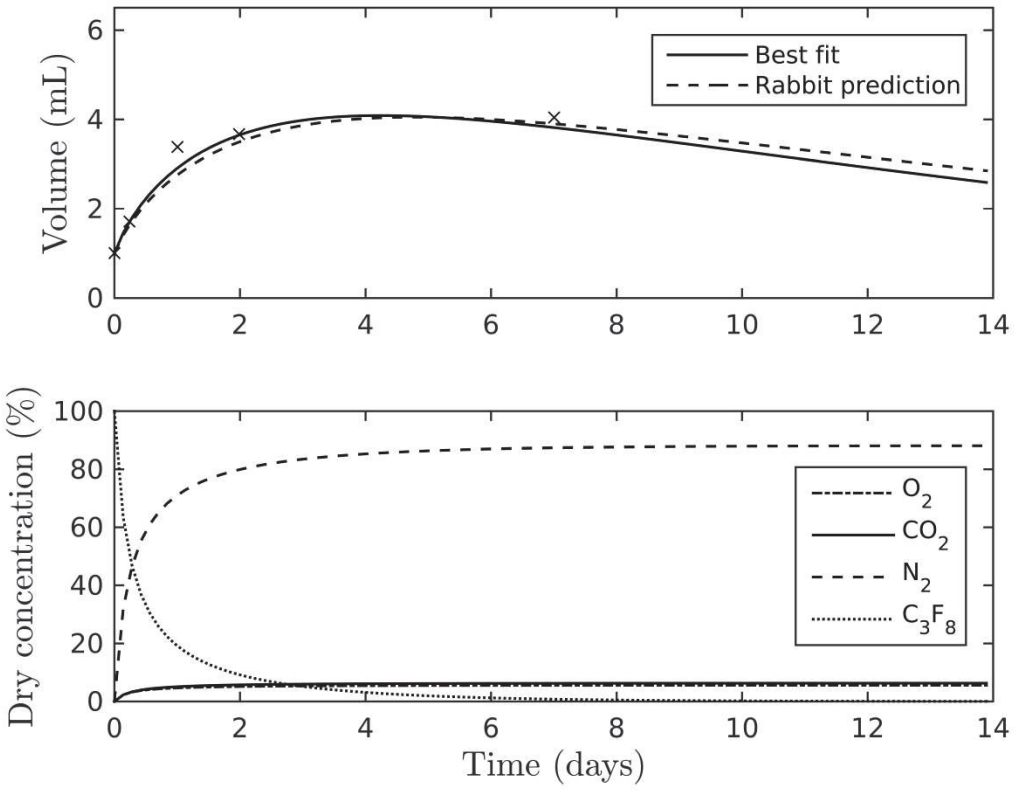

Figure 8A – Model prediction for the human C_3F_8 retinopexy case (100% C_3F_8, 1.0 mL injection) (Jacobs 1988). The prediction was based on rabbit mass transfer coefficients fitted to the data from Lincoff 1984. The rabbit predictions are shown by the dashed line, the best fit to the human data is shown by a solid line.

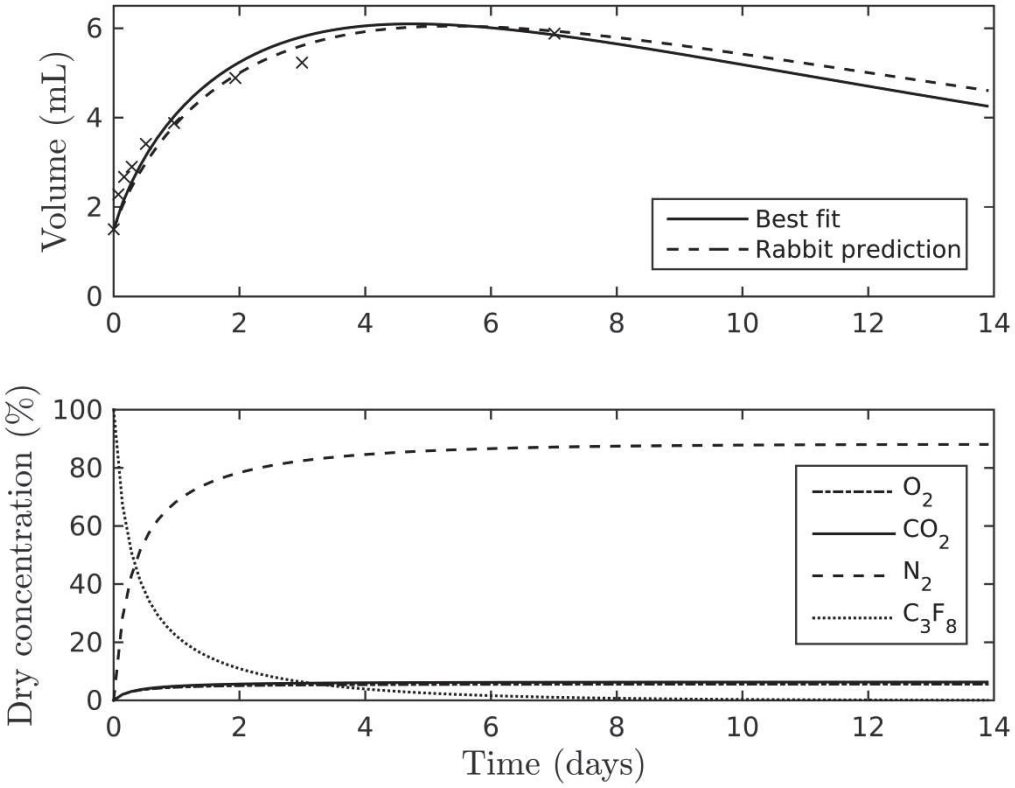

Figure 8B – Model prediction for the human C_3F_8 retinopexy case (100% C_3F_8, 1.5 mL injection) (Jacobs 1988). The prediction was based on rabbit mass transfer coefficients fitted to the data from Lincoff 1984. The rabbit predictions are shown by the dashed line, the best fit to the human data is shown by a solid line.

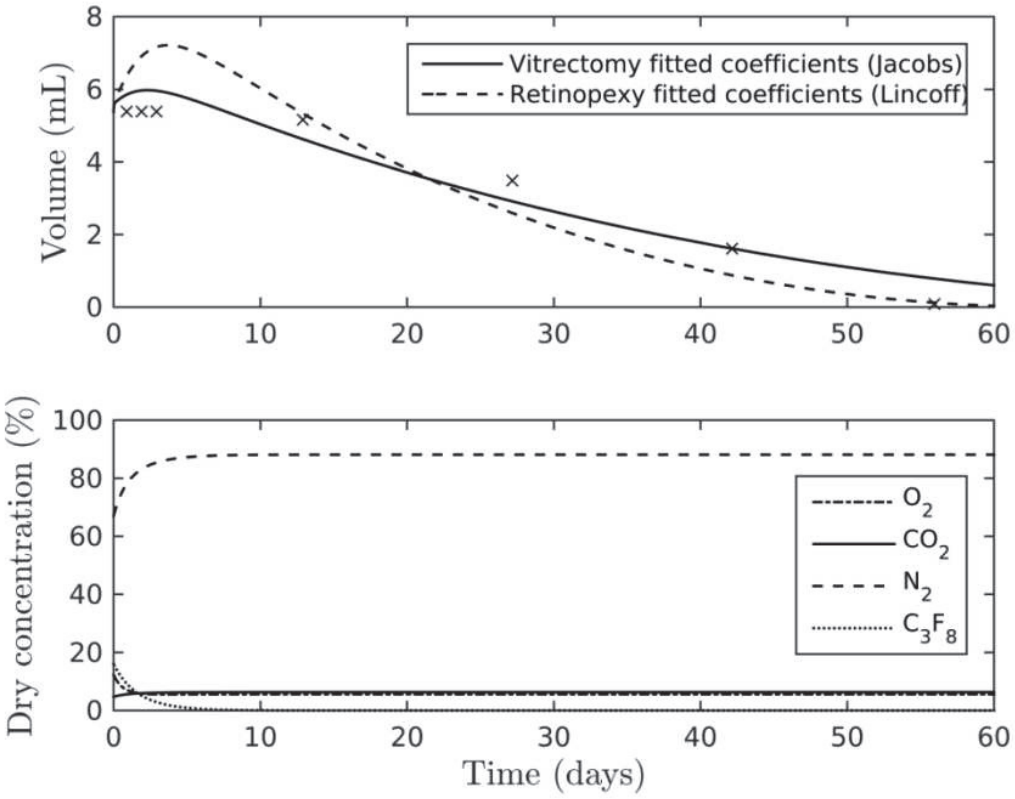

Figure 9 – Model prediction for the human C_3F_8 vitrectomy case (16% C_3F_8, balance air) (Jacobs 1988). The volumes reported at time zero were not used since these numbers were based on estimates and not a direct experimental measurement. (k_x = 1.32 x 10^{-8}, k_{O2}= 3.45 x 10^{-8} mol/cm2-day-mmHg)

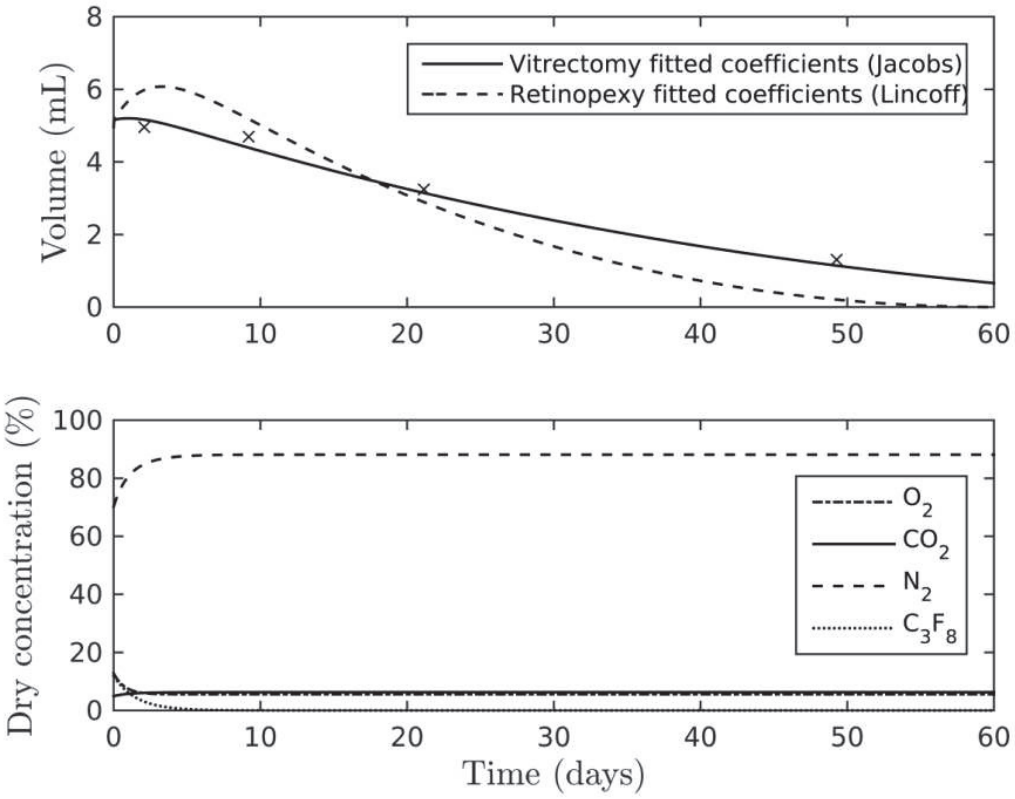

Figure 10 – Model prediction for the human C_3F_8 non-expansive vitrectomy case (12% C_3F_8, balance air) (Jacobs 1988). The literature reports non-expansive concentrations of 12 – 14% for C_3F_8. (Notice Acreole & Chang) The volumes reported at time zero were not used since these numbers were based on estimates and not a direct experimental measurement. (k_x = 1.50 x 10^{-8}, k_{O2}= 2.98 x 10^{-8} mol/cm2-day-mmHg)

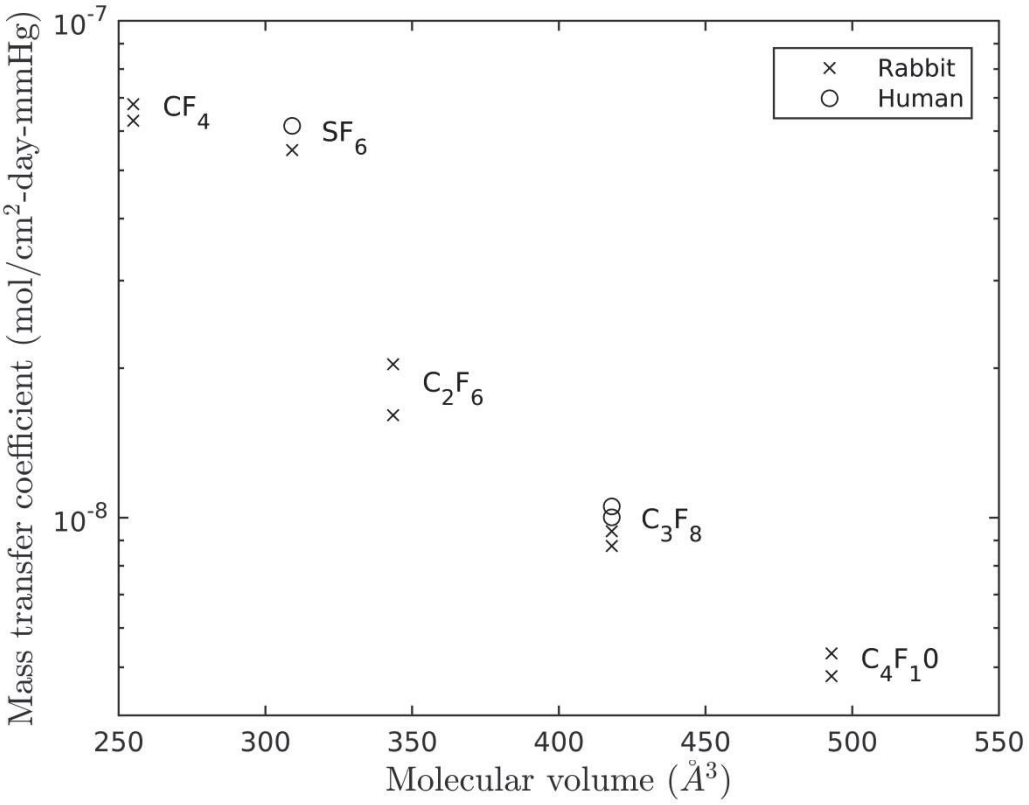

Figure 11A – Tamponade transfer coefficient (pneumatic retinopexy) against molecular volume for tamponade gas. This was fitted to Abrams (lune model), Lincoff ref (lune model) and Jacobs ref (spherical model).

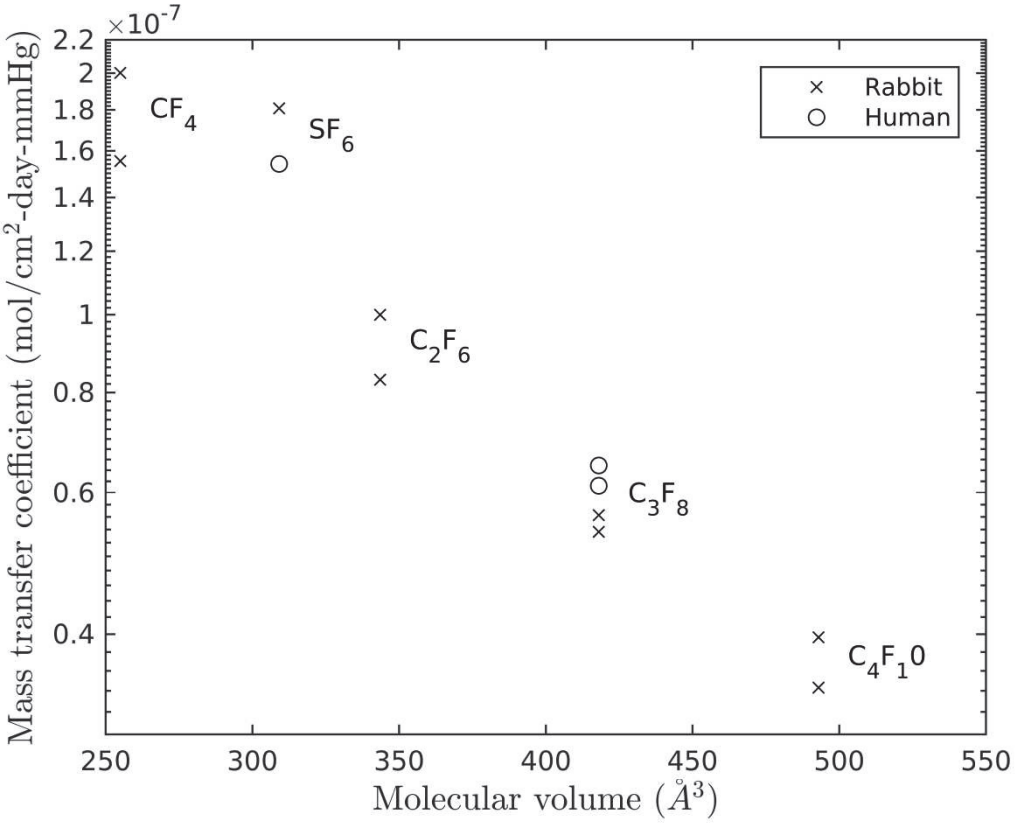

Figure 11B – Oxygen transfer coefficient (pneumatic retinopexy) against molecular volume. This was fitted to Abrams (lune model), Lincoff (lune model) and Jacobs (spherical model).

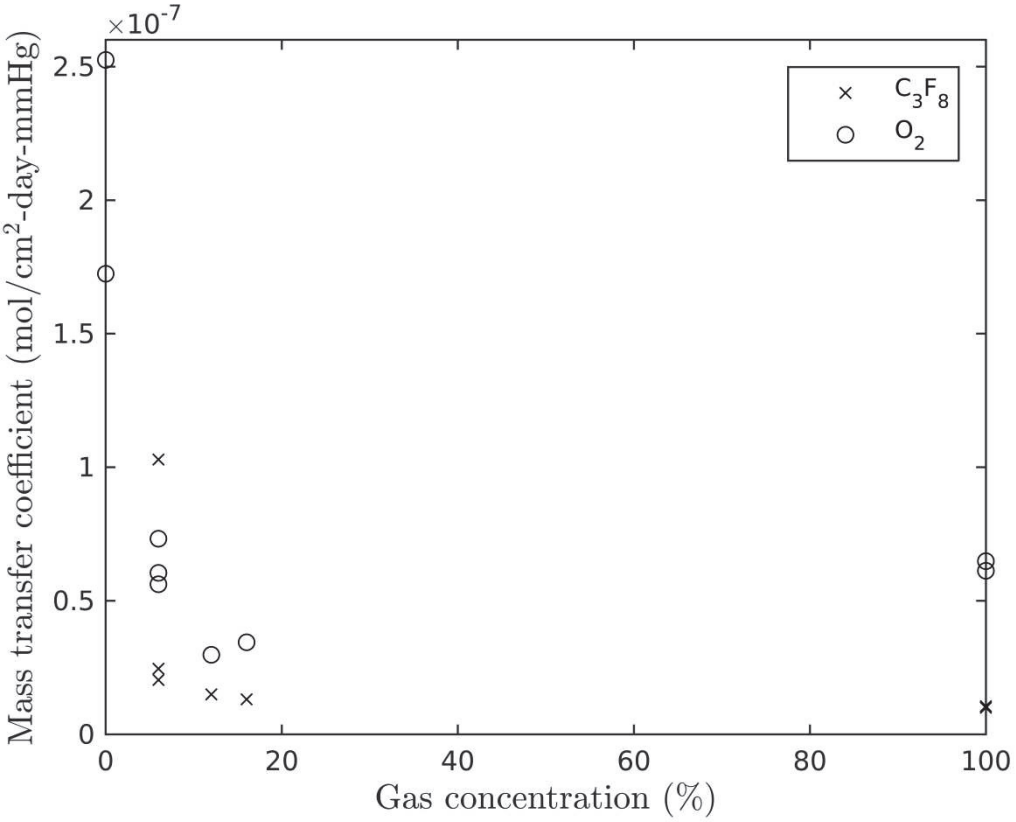

Figure 12 – C_3F_8 and oxygen mass transfer coefficients vs. initial tamponade gas composition, humans.